

Original Article
Medical Imaging



Cerebrospinal fluid flow in normal beagle dogs analyzed using magnetic resonance imaging

Hyunju Cho , Yejin Kim , Saebyel Hong , Hojung Choi *

Research Institute of Veterinary Medicine, College of Veterinary Medicine, Chungnam National University, Daejeon 34134, Korea

 OPEN ACCESS

Received: Sep 8, 2020

Revised: Oct 29, 2020

Accepted: Nov 5, 2020

*Corresponding author:

Hojung Choi

Research Institute of Veterinary Medicine,
College of Veterinary Medicine, Chungnam
National University, 99 Daehak-ro, Yuseong-
gu, Daejeon 34134, Korea
E-mail: hjchoi@cnu.ac.kr


© 2021 The Korean Society of Veterinary
Science

This is an Open Access article distributed
under the terms of the Creative Commons
Attribution Non-Commercial License ([https://
creativecommons.org/licenses/by-nc/4.0](https://creativecommons.org/licenses/by-nc/4.0))
which permits unrestricted non-commercial
use, distribution, and reproduction in any
medium, provided the original work is properly
cited.


ORCID iDs

Hyunju Cho 


<https://orcid.org/0000-0003-0967-1890>

Yejin Kim 

<https://orcid.org/0000-0002-5728-1320>

Saebyel Hong 

<https://orcid.org/0000-0003-2772-0465>

Hojung Choi 

<https://orcid.org/0000-0001-7167-0755>

Funding

This work was supported by research fund of
Chungnam National University.

Conflict of Interest

The authors declare no conflicts of interest.

Author Contributions

Conceptualization: Cho H. Data curation: Kim
Y, Hong S. Formal analysis: Cho H, Kim Y, Hong

ABSTRACT

Background: Diseases related to cerebrospinal fluid flow, such as hydrocephalus, syringomyelia, and Chiari malformation, are often found in small dogs. Although studies in human medicine have revealed a correlation with cerebrospinal fluid flow in these diseases by magnetic resonance imaging, there is little information and no standard data for normal dogs.

Objectives: The purpose of this study was to obtain cerebrospinal fluid flow velocity data from the cerebral aqueduct and subarachnoid space at the foramen magnum in healthy beagle dogs.

Methods: Six healthy beagle dogs were used in this experimental study. The dogs underwent phase-contrast and time-spatial labeling inversion pulse magnetic resonance imaging. Flow rate variations in the cerebrospinal fluid were observed using sagittal time-spatial labeling inversion pulse images. The pattern and velocity of cerebrospinal fluid flow were assessed using phase-contrast magnetic resonance imaging within the subarachnoid space at the foramen magnum level and the cerebral aqueduct.

Results: In the ventral aspect of the subarachnoid space and cerebral aqueduct, the cerebrospinal fluid was characterized by a bidirectional flow throughout the cardiac cycle. The mean \pm SD peak velocities through the ventral and dorsal aspects of the subarachnoid space and the cerebral aqueduct were 1.39 ± 0.13 , 0.32 ± 0.12 , and 0.76 ± 0.43 cm/s, respectively.

Conclusions: Noninvasive visualization of cerebrospinal fluid flow movement with magnetic resonance imaging was feasible, and a reference dataset of cerebrospinal fluid flow peak velocities was obtained through the cervical subarachnoid space and cerebral aqueduct in healthy dogs.

Keywords: Cerebrospinal fluid; dogs; magnetic resonance imaging

INTRODUCTION

The cerebrospinal fluid (CSF) is a liquid that fills the ventricles, central canals, and subarachnoid spaces (SAS). It is produced in the choroid plexus and brain parenchyma and is absorbed from the arachnoid villi. CSF removes waste and solvents and keeps the fragile brain tissue floating in buoyancy to maintain its shape and protect against external shocks [1-3]. CSF circulation is divided into 2 types of motion. The first is bulk flow, which is based on a hydrostatic pressure gradient primarily between the choroid plexus and arachnoid granulations. It is slow enough to be difficult to recognize using magnetic resonance imaging

S. Investigation: Choi H. Writing - original draft:
Cho H. Writing - review & editing: Choi H.

(MRI). In contrast, pulsatile flow is more likely to be detected on MRI because it is faster than bulk flow. It is based on the Monroe-Kellie doctrine, which states that the sum of blood, CSF, and brain parenchyma volumes is constant, limited by the volume of the skull. Thus, during contraction of the heart, CSF shows backward flow. Conversely, it moves forward during diastole of the heart [4].

Phase-contrast (PC) MRI is a specific sequence used for imaging CSF flow. It generates a signal contrast between flowing and stationary nuclei by sensitizing the phase of the transverse magnetization to the velocity of motion [5-7]. A key aspect of PC-MRI is the bipolar gradient, which is placed after the radiofrequency pulse and before data collection during echo time (TE). The principle of the bipolar gradient is to develop a phase shift of spins moving with a specific velocity along the direction of the axis [4]. PC-magnetic resonance (MR) images consist of the initial magnitude images, which represent flowing CSF as a bright signal and stationary tissues as a black background, and the subsequent phase-shift-encoded images with white and black signals representing forward and backward flows, respectively. Because of their phase-dependence, these images contain velocity information, which can be quantitatively estimated. Thus, CSF flow during the cardiac cycle may be displayed as a cine loop. Currently, PC-MRI is the best-known method and the only technique for both qualitative and quantitative assessment in clinical scenarios such as differential diagnosis and postsurgical follow-up [4]. However, this technique is limited by its poor visualization of turbulent flow and the inability to measure bulk flow [8-10].

Another sequence that can complement PC-MRI is time-spatial labeling inversion pulse (Time-SLIP). This is a variant of arterial spin-labeling that produces high-quality angiograms. The application of arterial spin-labeling lends itself very well to imaging CSF movement by using CSF as its own tracer. This approach can detect not only pulsatile flow but also bulk flow in slow-flowing regions. Unlike PC-MRI, quantitative evaluation is not possible with this technique, but it offers the advantage of a high signal-to-noise ratio and provides additional information about CSF flow patterns [11]. On the basis of the results of initial baseline studies, Time-SLIP can be readily used as a screening tool to determine whether the CSF flow is typical, atypical, or absent [12].

In human medicine, there are many reports that have attempted to assess CSF flow-related pathophysiology by measuring velocity and visualizing the flow of CSF with MRI. In one study, normal-pressure hydrocephalus patients showed a significantly higher peak systolic velocity of CSF than the control group [13]. Another study revealed a shorter systolic flow period of the temporal waveform for patients with communicating hydrocephalus in comparison with healthy controls [14]. For normal volunteers, the peak systolic velocities in the SAS at the foramen magnum level were measured. In symptomatic patients with Chiari I, peak systolic velocity was significantly higher than those in control volunteers [15], and CSF flow was characterized by flow jets, regions with a preponderance of flow in one direction, and synchronous bidirectional flow [16,17]. Additionally, one recent case report confirmed the patterns and directional changes of CSF flow in syringomyelia by using Time-SLIP [18].

Diseases associated with CSF flow were considered a rare condition in veterinary medicine, but they are now a relatively common neurologic diagnosis. Large ventricles are common findings in brachycephalic dog breeds [19]. Chiari-like malformations and syringomyelia are also often recognized in small-breed dogs. These changes can be attributed to the increased availability of MRI as well as the increased prevalence of these diseases in certain breeds,

most notably the Cavalier King Charles Spaniel [20]. Although there is still much debate about the underlying mechanisms and treatment methods, syringomyelia is also thought to be a consequence of abnormal CSF dynamics in dogs as in humans [21]. Therefore, based on the pathophysiology of these diseases, abnormalities of CSF flow are expected to appear in MR examinations in dogs.

In veterinary medicine, however, only one study has been conducted using MRI to evaluate and compare CSF flows. This previous study reported the patterns and velocities of CSF flow in Cavalier King Charles Spaniels with or without syringomyelia by using PC-MRI [22], but it assessed just five control dogs and obtained measurements only at the rear of the foramen magnum.

Therefore, in this experimental study, CSF flow velocity data was obtained from the cerebral aqueduct and SAS at the foramen magnum level using PC and Time-SLIP MRI in healthy beagle dogs. The purpose of this study was to provide baseline data of CSF flow velocity in dogs.

MATERIALS AND METHODS

Experimental animals

This experimental study was performed under the guidance of the Chungnam National University Animal Care and Use Committee (acceptance No.: 2019012A-CNU-189). Six beagle dogs (5 castrated males and 1 spayed female) with ages ranging from 2 to 7 years and weighing 7.7 to 11.5 kg (mean body weight: 9.3 ± 1.4 kg) were used for this study. For health status assessment of the dogs, physical and neurological examinations, laboratory analyses, including complete blood count, serum biochemical assessments, and imaging examinations, including skull, thoracic, and abdominal radiography, computed tomography (CT) of the head, and brain MRI, were performed. On the CT images, the bone window was obtained to evaluate the presence of caudal occipital malformation. T2-weighted fast spin-echo MR images were used to confirm the absence of other abnormalities in the brain parenchyma. When structural abnormalities and parenchymal lesions were not identified in these images, CSF flow assessment was carried out.

Anesthesia

All experimental animals were fasted for approximately 12 h and hydrated for 2 h before the MRI examination. Anesthesia was induced with 3.0 mg/kg of alfaxalone (Alfaxan® Inj.; Jurox Pharm. Co. Ltd., Australia). After intubation, anesthesia was maintained with isoflurane 1-2 MAC (Ifiran®, Hana Pharm, Korea) in oxygen. After the anesthesia began, the following vital signs were recorded every 5 min: temperature, heart rate, respiratory rate, blood pressure, capillary refill time (CRT), femoral pulse, and end-tidal CO₂. The dosage of drugs was recorded if additional drugs were used. MR sequences related to CSF flow were obtained only when the dog met the following conditions: heart rate, 60–120 beats per minute (bpm); end-tidal CO₂, 32–45 mmHg; and respiratory rate of 8–12. Blood pressure was assessed subjectively by an experienced veterinarian for anesthesia through evaluations of the CRT and femoral pulse.

MRI

MRI was performed using a 1.5-Tesla scanner (Vantage Elan™; Canon, Japan) with a combination of a 16-channel flexible coil and spine coil. All dogs were positioned in ventral

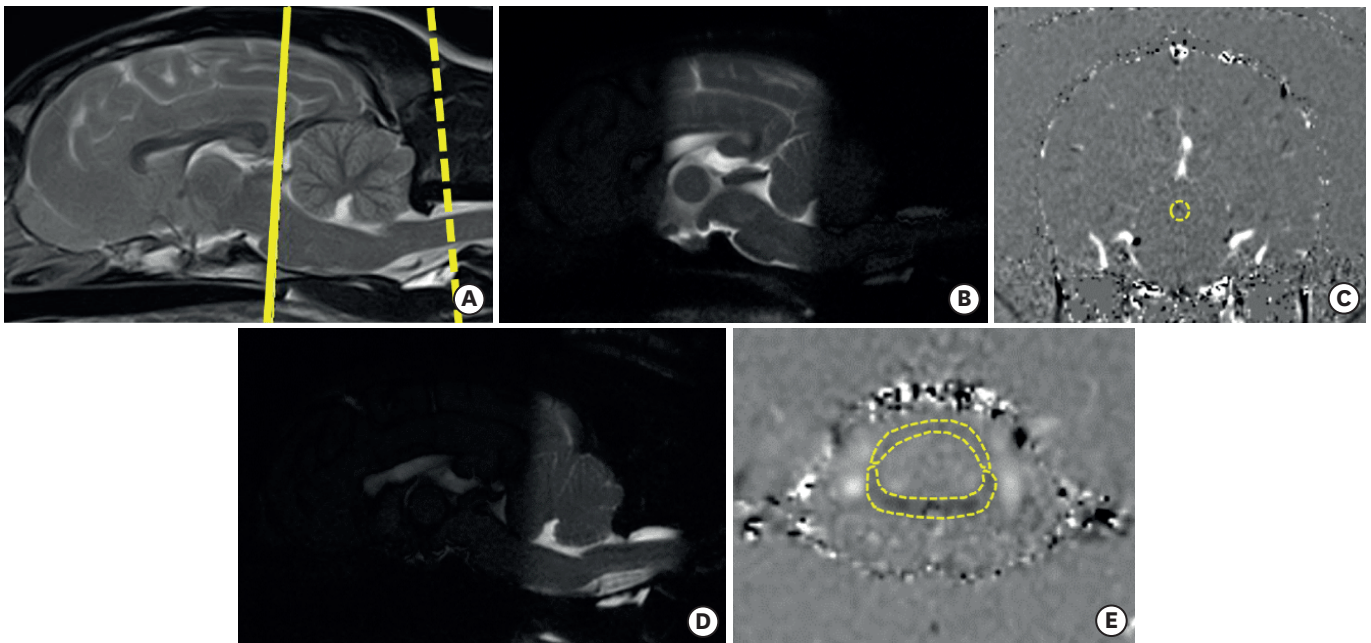


Fig. 1. A sagittal T2W image showing the cerebral aqueduct level (solid line) and foramen magnum level (dashed line) (A). Time-SLIP sagittal plane images and PC-MR transverse plane images at the cerebral aqueduct (B,C) and foramen magnum level (D,E). As shown in the (C and E), measurements are made in 3 ROIs; cerebral aqueduct and the dorsal and ventral aspects of the SAS. T2W, T2 weighted; Time-SLIP, time-spatial labeling inversion pulse; PC, phase-contrast; MR, magnetic resonance; ROIs, regions of interest; SAS, subarachnoid spaces.

recumbency, with the cerebellum at the center of the two coils. In addition to the spine coils, the flexible coil was wrapped around the dogs' heads to enhance the quality of the images acquired.

CSF flow scanning was performed using Time-SLIP and PC imaging. These two sequences were taken at 2 levels: the foramen magnum and the cerebral aqueduct level (**Fig. 1**).

Preferentially, Time-SLIP images with various inversion times (TIs) were obtained 20 times at a TI increment of 50 ms, starting from 1,000 to 1,950 ms. The labeling pulse had a thickness of 5 cm and was placed to include one scan level. Next, referring to the Time-SLIP images, the transverse section showing the CSF flow in PC-MR imaging was selected. A cine acquisition with sensitivity to velocity in the section-select direction was obtained on a transverse plane of the section perpendicular to the aqueduct and SAS. A cardiac-gated flow-compensated gradient echo sequence with flow velocity encoding of 8 cm/s in the slice-selective direction was used with the following parameters: repetition time (TR)/TE, 24 ms/10 ms; phases, 25; flip angle, 20°; field of view, 11 × 11 cm; matrix, 256 × 256; and slice thickness, 4 mm. The mean image acquisition times were 15 min 10 sec and 5 min 26 sec, respectively, for Time-SLIP and PC-MRI.

Evaluation and measurement

Time-SLIP

Time-SLIP analysis shows a direct visualization of CSF flow and characterization of flow dynamics. Using a total of 20 images, each dog was assessed to show a basic flow pattern. If abnormal flow patterns such as bubbles, jumping, and fast flow were found, they were excluded from the experiment.

PC-MRI

Using the postprocessing technique on the MR system, the velocities could be obtained directly from the signal intensities. The regions of interest (ROIs) were drawn manually in areas where the signal changed depending on the CSF flow at the cine images by selecting free-form polygonal shapes for the SAS at the foramen magnum level and the oval shape for the cerebral aqueduct. The CSF velocity was measured at three locations: the ventral and dorsal aspects of the SAS at the foramen magnum level and cerebral aqueduct (**Fig. 1**). In every sequence, CSF was scanned at 24-ms intervals from 0 to 576 ms, yielding 25 values. This process was repeated four times with an interval. This quantitative assessment of CSF flow using manual ROI placement was performed by three independent readers with 2 years of experience in veterinary medical imaging.

The velocity measurement data for the CSF were analyzed using 2 methods. The first involved investigation of waveforms at CSF flow velocities over time for each ROI. The other method statistically calculated the CSF velocity values by the location of the ROIs.

Statistical analysis

CSF flow velocity measurements were obtained for all dogs. The peak velocities within three ROIs were measured and compared with each other. Mean velocities, within-subject SD, intra- and interclass correlation coefficients (ICCs) were calculated. For all analyses, a *p* value < 0.05 was considered statistically significant. All statistics were performed using a computer statistical package (Statistics Package for the Social Science, ver. 24; SPSS Inc., USA).

RESULTS

PC-MR and Time-SLIP imaging were successfully performed in all dogs over a full study period lasting approximately 40 min/dog. CSF flow was detected in all ROIs, and velocity measurements were obtained.

Time-SLIP

The signal changes indicating CSF movement in the SAS and cerebral aqueduct were displayed as a cine loop, which was converted into color to obtain better performance with the postprocessing technique on the MR system (**Fig. 2**). In the conversion image, red and green represent the bright regions in the primary image, which is interpreted as tagged CSF. In this experiment, the range of red areas was shown to be increased in the dorsal SAS and cerebral aqueduct. In the ventral SAS, tagged CSF was observed extending the caudal part with a decrease and increase in green areas.

PC-MRI

The mean waveforms of 6 dogs' CSF flow studies were plotted with velocities in centimeters per second on the y-axis and fractions of the cardiac cycle on the x-axis (**Fig. 3**). The positive deflections represent the craniocaudal flow, and the negative deflections represent caudocranial flow.

In the ventral part of the cervical SAS and cerebral aqueduct, the CSF was characterized by bidirectional flow throughout the cardiac cycle. This can be seen by the time point of zero velocity, which indicates a change in the direction of CSF flow and was noted twice and three times, respectively. The point at which positive values begin after the R wave indicates

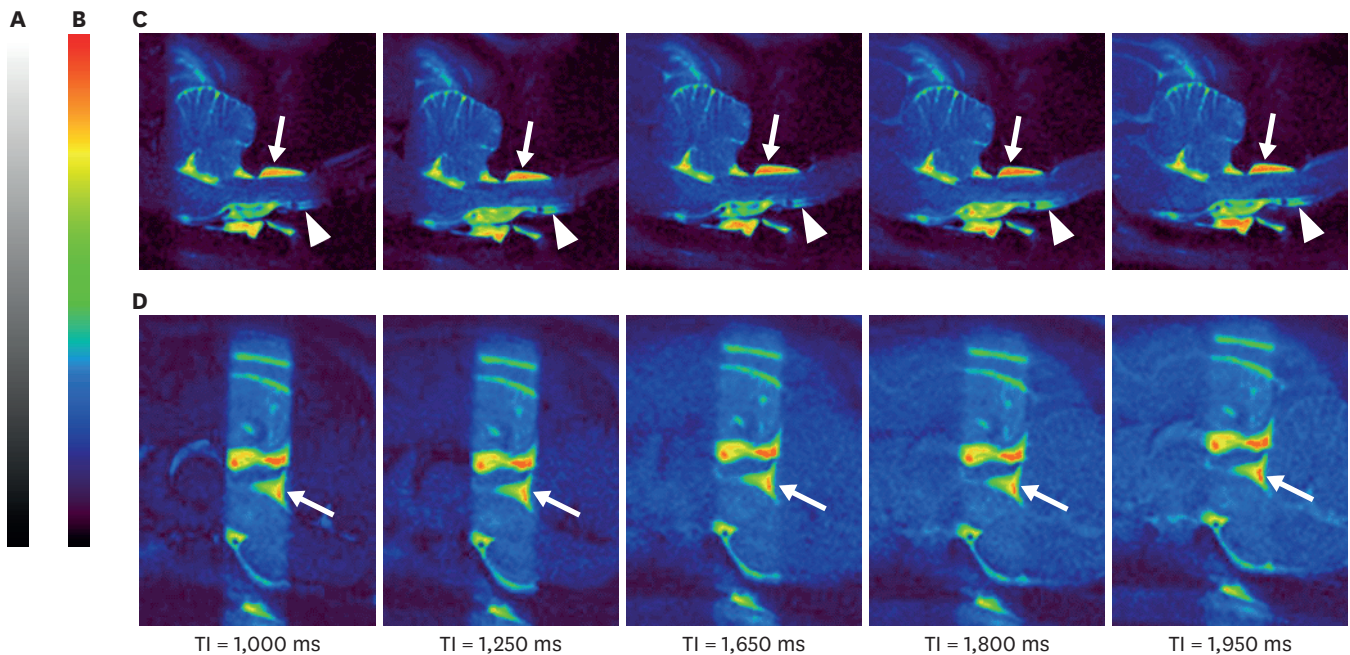


Fig. 2. Sagittal Time-SLIP MR images after a transverse labeling pulse show the contrast difference between tagged and untagged CSF at various TIs. The image is converted to color to maximize the expression of light and shade. Scale bar of primary images (A) and converted images (B). Labeled CSF in the cervical arachnoid space (C) and cerebral aqueduct (D) enters the caudal SAS and 4th ventricle. The red and green areas, indicating tagged CSF, increase in the dorsal SAS and cerebral aqueduct (arrows). In addition, in the ventral SAS, the green areas are seen extending backwards (arrow heads). Time-SLIP, time-spatial labeling inversion pulse; MR, magnetic resonance; CSF, cerebrospinal fluid; TI, inversion time; SAS, subarachnoid spaces.

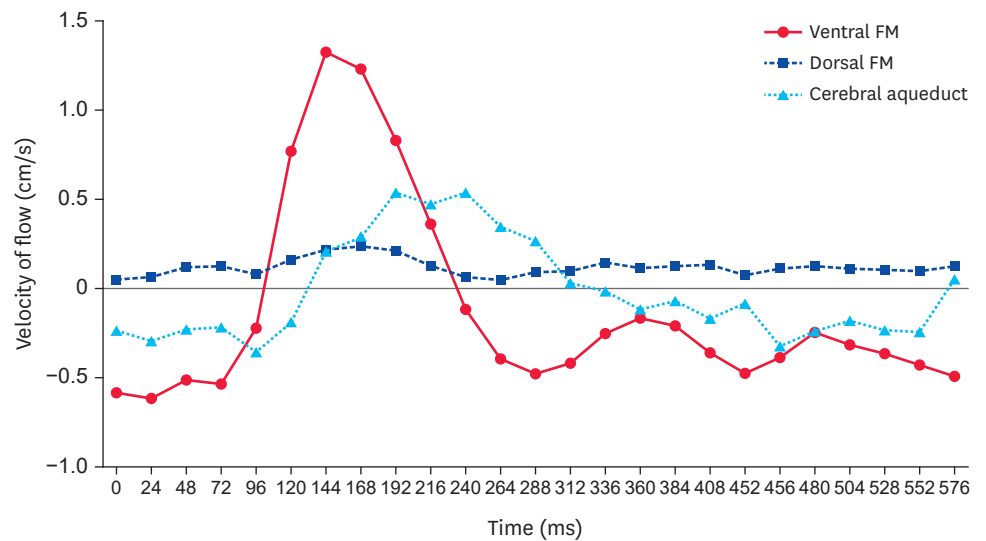


Fig. 3. CSF flow waveforms of 6 dogs in three ROIs. The positive deflections represent craniocaudal flow and the negative deflections represent caudocranial flow. FM, foramen magnum; CSF, cerebrospinal fluid; ROIs, regions of interest.

the start of the systolic period. This time tended to be faster in the ventral SAS than in the cerebral aqueduct. In both the ventral SAS and cerebral aqueduct, CSF flow waveforms were characterized by relatively narrow systolic peaks than the diastolic troughs. Therefore, the diastolic slopes were less steep than the systolic slopes. The systole duration was shorter than that of the diastole. The diastole duration could be measured at the point where the third zero point in the CSF waveform at the cerebral aqueduct begins with the second contraction

Table 1. Peak CSF flow velocity of 6 Beagle dogs at three ROIs on PC-MRI.

Dog	Peak CSF flow velocity (cm/s)		
	Ventral SAS at the FM level	Dorsal SAS at the FM level	Cerebral aqueduct
1	1.46	0.30	0.87
2	1.17	0.27	1.60
3	1.52	0.32	0.47
4	1.40	0.33	0.54
5	1.41	0.53	0.56
6	1.39	0.17	0.48
Mean	1.39 ^a	0.32 ^a	0.76 ^a
SD	0.13	0.12	0.43
95% CI	1.34–1.44	0.28–0.37	0.61–0.94

The results measured four times for each location were averaged both individually and totally.

CSF, cerebrospinal fluid; ROIs, regions of interest; PC, phase-contrast; MRI, magnetic resonance imaging; SAS, subarachnoid space; FM, foramen magnum; CI, confidence interval.

^ap < 0.001 compared to other ROI locations.

Table 2. Intra- and inter-observer agreement evaluation of peak velocity at 3 ROIs

	Ventral SAS at the FM level	Dorsal SAS at the FM level	Cerebral aqueduct
ICC (Intra-observer)	0.900	0.970	0.974
ICC (Inter-observer)	0.841	0.900	0.822

Reliability level: 0.800–1.000 (high reliability), 0.600–0.790 (moderate reliability), and ≤ 0.590: (unreliable). ROIs, regions of interest; SAS, subarachnoid space; FM, foramen magnum; ICC, intra- or inter-observer correlation coefficient.

of the heart. However, the waveform in the ventral SAS was assumed to be greater than that since the third zero point did not appear within 576 ms. On the other hand, the waveform in the dorsal SAS revealed no greater to-and-fro movement than anywhere else. Moreover, it showed a tendency to flow steadily at a similar flow rate in the present study.

The mean ± SD peak velocity was 1.39 ± 0.13 cm/s through the ventral aspect of the SAS, 0.32 ± 0.12 cm/s through the dorsal aspect of the SAS, and 0.76 ± 0.43 cm/s through the cerebral aqueduct. The peak velocities at each region differed significantly from each other. The values for each dog are summarized with their respective 95% confidence intervals in **Table 1**.

The results were analyzed on the basis of ICCs (**Table 2**). The assessments confirmed that the repeated measurements were reliable. ROIs at all locations also showed high agreement in the analysis of the inter-observer agreement.

DISCUSSION

In this study, it was possible to assess CSF flow in all dogs by using Time-SLIP and PC-MR imaging, allowing noninvasive quantitative evaluation of velocity and qualitative evaluation of the flow pattern. First, by using the time-SLIP technique, we investigated whether it was possible to identify communication between the CSF spaces. We also could get a velocity values measured using PC-MRI. In addition, it was confirmed that the flow showed a normal reflux pattern, not a turbulent flow that can be seen in an abnormal state on PC-MR images.

The CSF velocity values were compared with those in a previous veterinary study [22] conducted on 59 animals with neurological symptoms of the Cavalier King Charles Spaniel breed, which is predisposed to Chiari malformations that are responsible for syringomyelia. For comparison, four beagles and one mixed dog were included in the control group. The measurement locations for the analysis were foramen magnum level, with the mean of peak

velocities for the ventral and dorsal aspects of SAS, based on normal dogs included in the control group, being 0.75 ± 0.24 cm/s and 0.59 ± 0.13 cm/s, respectively. Their results were not consistent with ours. This discrepancy may be attributable to multiple factors including scan parameters, the positional difference of the neck, anesthetic agents, and location and size of ROIs. Infants are known to have higher CSF flow velocities than adults in humans. This is thought to be due to arterial pulse wave variations with age [23]. Since both the previous and present studies used adult dogs, age would not have affected the results. Studies assessing the effects of breed and/or body weight on CSF flow have not yet been performed, but since dogs of similar breed and body weight were used, these factors also cannot explain the differences in results. In addition, we controlled the heart rate to ensure CSF flow within a range of 60–120 bpm, as in the previous study.

A CSF flow pattern of to-and-fro movement resulting from heart contraction and relaxation was observed in the ventral SAS and cerebral aqueduct. Humans have been reported show pulsatile waves in both the dorsal and ventral SAS, but some normal individuals may also show loss of this movement. In this study, there was no clear contrast change in the dorsal SAS at the time of drawing ROIs for measurement in PC-MR images, and no obvious to-and-fro movement was observed during the measurement as a result. This may be due to the head angle. In a previous study, the head angle was set in the range of 100° to 138° in a similar standing position. In this experiment, however, the dogs were positioned in basic ventral recumbency without flexion of the neck. This may have made the dorsal SAS smaller than the neck flexed position [22]. In fact, Sofia et al. also claimed that when scanned with the neck in extension and in flexion, the dorsal aspect of the SAS was particularly large in the flexion state.

Although the effects of changes in CSF flow from drugs have not yet been shown, anesthetics are thought to change physiological conditions directly related to CSF flow, such as heart rate and blood pressure. In a previous study [22], each dog was premedicated with fentanyl, and anesthesia was induced with propofol and maintained using inhaled sevoflurane. Since these drugs do not match the anesthetic drugs in the current study, it is assumed that the results may change. Alfaxalone, which was used for anesthesia in this experiment, is known to produce dose-dependent changes in the cardiovascular system [24]. According to previous studies, transient tachycardia and hypotensive effects have been noted immediately after drug administration when larger doses are administered [25]. Although this effect is minimal at a dose of less than 6 mg/kg [24], it is impossible to say that there was no effect in this experiment. In this respect, the subjective measurement of blood pressure in this experiment is a limitation.

It is important to consider that, depending on the situation, variations can be introduced by the measurement method. Plane selection and manual ROI placement in relation to the anatomic region are also known to affect the overall obtained values. In particular, for very narrow aqueducts, this error may be even higher because noise and poor contrast make the placement of the ROI difficult [26]. The flow in the center is higher than at the periphery, so a small ROI placed in the center of the aqueduct will yield higher readings of mean velocity, and a larger ROI will underestimate it. However, the peak velocity representing the fastest flow in any pixel in the given ROI is not affected by the ROI size [13].

One limitation of PC-MRI is that proper setting of the recording time is required through adjustment of TR and phase number. Since the heart rate of dogs is approximately twice that of humans, TR and recording time were set at half values. However, in the ventral SAS, it

was difficult to measure the exact duration of the diastole period because the second onset of systole was not recorded. Therefore, the findings are thought to be more accurate if the recording time is set such that it can be increased. Also, this study was performed only in same purpose-bred dogs with similar size.

A uniform relative evaluation is difficult because each individual has a different heart rate, measured ROI, etc., and there is no method to analyze the amount of CSF produced, but it is thought to be meaningful in understanding the direction of the overall circulation. The results of this study confirmed that normal net flow rate/cycle would, in most cases, flow positive from the third to the fourth ventricle.

In conclusion, studies of CSF circulation using MRI with visible images of CSF circulation are a useful method for understanding CSF flow dynamics. We obtained a reference data set of CSF flow peak velocities through the cervical SAS and cerebral aqueduct in healthy dogs. This approach is thought to be especially important considering the possibility of various errors occurring in these assessments. Therefore, specific guidelines for CSF MR examination are crucial to obtain comparable and reliable data across different studies. In that sense, the results of this study provide valuable data for future research on CSF flow disorders such as hydrocephalus, Chiari-like malformation, and syringohydromyelia. A large-scale future study is also needed to establish a standard technique for normal CSF flow in the future.

REFERENCES

1. Segal MB, Pollay M. The secretion of cerebrospinal fluid. *Exp Eye Res.* 1977;25 Suppl:127-148.
[PUBMED](#) | [CROSSREF](#)
2. Pollay M. The function and structure of the cerebrospinal fluid outflow system. *Cerebrospinal Fluid Res.* 2010;7(1):9.
[PUBMED](#) | [CROSSREF](#)
3. Sakka L, Coll G, Chazal J. Anatomy and physiology of cerebrospinal fluid. *Eur Ann Otorhinolaryngol Head Neck Dis.* 2011;128(6):309-316.
[PUBMED](#) | [CROSSREF](#)
4. Korbecki A, Zimny A, Podgórski P, Szaśiadek M, Bładowska J. Imaging of cerebrospinal fluid flow: fundamentals, techniques, and clinical applications of phase-contrast magnetic resonance imaging. *Pol J Radiol.* 2019;84:e240-e250.
[PUBMED](#) | [CROSSREF](#)
5. Dumoulin CL, Yucel EK, Vock P, Souza SP, Terrier F, Steinberg FL, et al. Two- and three-dimensional phase contrast MR angiography of the abdomen. *J Comput Assist Tomogr.* 1990;14(5):779-784.
[PUBMED](#) | [CROSSREF](#)
6. Tsuruda JS, Shimakawa A, Pelc NJ, Saloner D. Dural sinus occlusion: evaluation with phase-sensitive gradient-echo MR imaging. *AJNR Am J Neuroradiol.* 1991;12(3):481-488.
[PUBMED](#)
7. Quencer RM, Post MJ, Hinks RS. Cine MR in the evaluation of normal and abnormal CSF flow: intracranial and intraspinal studies. *Neuroradiology.* 1990;32(5):371-391.
[PUBMED](#) | [CROSSREF](#)
8. Malko JA, Hoffman JC Jr, McClees EC, Davis PC, Braun IF. A phantom study of intracranial CSF signal loss due to pulsatile motion. *AJNR Am J Neuroradiol.* 1988;9(1):83-89.
[PUBMED](#)
9. Sherman JL, Citrin CM, Gangarosa RE, Bowen BJ. The MR appearance of CSF flow in patients with ventriculomegaly. *AJR Am J Roentgenol.* 1987;148(1):193-199.
[PUBMED](#) | [CROSSREF](#)
10. Wagshul ME, Chen JJ, Egnor MR, McCormack EJ, Roche PE. Amplitude and phase of cerebrospinal fluid pulsations: experimental studies and review of the literature. *J Neurosurg.* 2006;104(5):810-819.
[PUBMED](#) | [CROSSREF](#)

11. Yamada S, Tsuchiya K, Bradley WG, Law M, Winkler ML, Borzage MT, et al. Current and emerging MR imaging techniques for the diagnosis and management of CSF flow disorders: a review of phase-contrast and time-spatial labeling inversion pulse. *AJNR Am J Neuroradiol.* 2015;36(4):623-630.
[PUBMED](#) | [CROSSREF](#)
12. Yamada S, Miyazaki M, Kanazawa H, Higashi M, Morohoshi Y, Bluml S, et al. Visualization of cerebrospinal fluid movement with spin labeling at MR imaging: preliminary results in normal and pathophysiologic conditions. *Radiology.* 2008;249(2):644-652.
[PUBMED](#) | [CROSSREF](#)
13. Tawfik AM, Elsorogy L, Abdelghaffar R, Naby AA, Elmenshawi I. Phase-contrast MRI CSF flow measurements for the diagnosis of normal-pressure hydrocephalus: observer agreement of velocity versus volume parameters. *AJR Am J Roentgenol.* 2017;208(4):838-843.
[PUBMED](#) | [CROSSREF](#)
14. Balédent O, Gondry-Jouet C, Meyer ME, De Marco G, Le Gars D, Henry-Feugeas MC, et al. Relationship between cerebrospinal fluid and blood dynamics in healthy volunteers and patients with communicating hydrocephalus. *Invest Radiol.* 2004;39(1):45-55.
[PUBMED](#) | [CROSSREF](#)
15. Haughton VM, Korosec FR, Medow JE, Dolar MT, Iskandar BJ. Peak systolic and diastolic CSF velocity in the foramen magnum in adult patients with Chiari I malformations and in normal control participants. *AJNR Am J Neuroradiol.* 2003;24(2):169-176.
[PUBMED](#)
16. Quigley MF, Iskandar B, Quigley ME, Nicosia M, Haughton V. Cerebrospinal fluid flow in foramen magnum: temporal and spatial patterns at MR imaging in volunteers and in patients with Chiari I malformation. *Radiology.* 2004;232(1):229-236.
[PUBMED](#) | [CROSSREF](#)
17. Iskandar BJ, Quigley M, Haughton VM. Foramen magnum cerebrospinal fluid flow characteristics in children with Chiari I malformation before and after craniocervical decompression. *J Neurosurg.* 2004;101(2 Suppl):169-178.
[PUBMED](#) | [CROSSREF](#)
18. Takeuchi K, Ono A, Hashiguchi Y, Misawa H, Takahata T, Teramoto A, et al. Visualization of cerebrospinal fluid flow in syringomyelia through noninvasive magnetic resonance imaging with a time-spatial labeling inversion pulse (Time-SLIP). *J Spinal Cord Med.* 2017;40(3):368-371.
[PUBMED](#) | [CROSSREF](#)
19. Laubner S, Ondreka N, Failing K, Kramer M, Schmidt MJ. Magnetic resonance imaging signs of high intraventricular pressure—comparison of findings in dogs with clinically relevant internal hydrocephalus and asymptomatic dogs with ventriculomegaly. *BMC Vet Res.* 2015;11(1):181.
[PUBMED](#) | [CROSSREF](#)
20. Rusbridge C, Knowler SP. Inheritance of occipital bone hypoplasia (Chiari type I malformation) in Cavalier King Charles Spaniels. *J Vet Intern Med.* 2004;18(5):673-678.
[PUBMED](#) | [CROSSREF](#)
21. Rusbridge C, Greitz D, Iskandar BJ. Syringomyelia: current concepts in pathogenesis, diagnosis, and treatment. *J Vet Intern Med.* 2006;20(3):469-479.
[PUBMED](#) | [CROSSREF](#)
22. Cerda-Gonzalez S, Olby NJ, Broadstone R, McCullough S, Osborne JA. Characteristics of cerebrospinal fluid flow in Cavalier King Charles Spaniels analyzed using phase velocity cine magnetic resonance imaging. *Vet Radiol Ultrasound.* 2009;50(5):467-476.
[PUBMED](#) | [CROSSREF](#)
23. Iskandar BJ, Haughton V. Age-related variations in peak cerebrospinal fluid velocities in the foramen magnum. *J Neurosurg.* 2005;103(6 Suppl):508-511.
[PUBMED](#) | [CROSSREF](#)
24. Muir W, Lerche P, Wiese A, Nelson L, Pasloske K, Whittem T. Cardiorespiratory and anesthetic effects of clinical and supraclinical doses of alfaxalone in dogs. *Vet Anaesth Analg.* 2008;35(6):451-462.
[PUBMED](#) | [CROSSREF](#)
25. Child KJ, Currie JP, Davis B, Dodds MG, Pearce DR, Twissell DJ. The pharmacological properties in animals of CT1341—a new steroid anaesthetic agent. *Br J Anaesth.* 1971;43(1):2-13.
[PUBMED](#) | [CROSSREF](#)
26. Lee JH, Lee HK, Kim JK, Kim HJ, Park JK, Choi CG. CSF flow quantification of the cerebral aqueduct in normal volunteers using phase contrast cine MR imaging. *Korean J Radiol.* 2004;5(2):81-86.
[PUBMED](#) | [CROSSREF](#)